Random sequential adsorption of polyatomic species on fractal substrates

V. Cornette,* A. J. Ramirez-Pastor, and F. Nieto
Departamento de Física, Instituto de Física Aplicada (INFAP), Universidad Nacional de San Luis, CONICET, Chacabuco 917, D5700BWS San Luis, Argentina

(Received 3 September 2010; revised manuscript received 30 March 2011; published 16 May 2011)

Random sequential adsorption of k-mers of different sizes and shapes deposited on two types of fractal surfaces (deterministic and statistical) is studied. These kinds of substrates present intrinsic heterogeneities. As a consequence, the average coordination number depends on the topology that characterizes the adsorbent. For discrete models, at the late stage the surface coverage evolves according to $\theta(t) = \theta_j - A\exp[-\frac{t}{\sigma}]$, where θ_j is the jamming coverage while A and σ are fitting parameters. A detailed analysis of how these main quantities $[\theta_j, \sigma]$ depend on the relationship between the geometry of the adsorbate and the adsorbent is presented. The results obtained suggest that the symmetry of the substrate may exert a decisive influence on the adsorption kinetics of polyatomic species.

DOI: 10.1103/PhysRevE.83.051119 PACS number(s): 02.50.Ey, 68.43.Mn, 02.70.Uu

I. INTRODUCTION

Random sequential adsorption (RSA) is one of the simplest and most efficient approaches to analyze sequences of irreversible events. A number of processes in physics, chemistry, and biology where the microscopic events occur irreversibly on the time scales of the experiments can be studied as RSA on a lattice. The approach of RSA has been used, among others, in models for reactions on polymer chains [1,2], chemisorption on crystal surfaces [3], adsorption in colloidal systems [4,5], random growth in surface physics [6], growth processes in three-dimensional (3D) solid-state physics [7,8], technology of composites [9], granular matter study [10], and disordered systems [11], and also in the wider context of ecology [12] or sociology [13].

RSA or irreversible deposition is a process in which the objects of a specified shape are randomly and sequentially deposited onto a substrate. The focus is on the monolayer deposition where depositing objects are not allowed to overlap. The adsorbed particles are permanently fixed at their spatial positions. Once an object is placed, it affects the geometry of all later placements, so the dominant effect in RSA is the blocking of the available substrate area. The deposition process ceases when all unoccupied spaces are smaller than the size of an adsorbed particle. The system is then jammed in a nonequilibrium disordered state for which the limiting (jamming) coverage θ_j is less than the corresponding density of closest packing. The kinetic properties of a deposition process are described by the time evolution of the coverage $\theta(t)$, which is the fraction of the substrate area occupied by the adsorbed particles. This dependence has been an object of analysis during recent decades. In previous theoretical studies of RSA, which include Monte Carlo approaches [14–18], series expansion [16,19,20], rate equations [15,17,21], etc., both continuous and discrete models were analyzed. In such studies, it was established that the late-stage deposition kinetics follows either a power law (for continuous models) or an exponential function (for discrete models) approach toward the jamming limit. Thus, for discrete models, one writes for long times,

$$\theta(t) = \theta_j - A\exp\left[-\frac{t}{\sigma}\right], \tag{1}$$

where θ_j is the jamming coverage while A and σ are fitting parameters. In particular, σ determines how fast the lattice is filled up to the jamming coverage.

From a practical point of view, the problem of particle deposition on heterogeneous surfaces seems to be especially interesting. Recently, much interest has been focused on heterogeneous surfaces bearing patterned surface features of a regular shape. Theoretical calculations have been performed for the ring-shaped patterned surfaces using the limiting trajectory [22] and the convective-diffusion approach [23]. Other contributions have studied RSA on the Cayley tree [24], while the kinetics of adsorptions of large spherically shaped molecules on nanopatterned substrates has been modeled by employing generalized versions of the RSA model [25].

Also, experimental measurements have been done for surface features having the form of circles and dots [26–28], squares [29–31], rectangles and stripes [32–37], and others [38]. Most real solid surfaces present a combination of two types of heterogeneities: (i) energetic heterogeneity manifested through the variation of adsorption energy from one site to another, and (ii) geometric heterogeneity associated with the existence of irregularities in the lattice of depositing sites. In the case of solids that present geometric heterogeneities, the use of fractals as depositing lattice has the advantage not only because their intrinsic self-similarity makes the problem more amenable to an exact approach, but also because these lattices as such may serve to model porous media. In most of the cases treated in the literature, the surface where the particles are deposited has been considered to be chemically homogeneous and smooth. However, (i) for many real systems, the most important physical properties depend on the detailed geometry of the substrate, and (ii) in contrast to the statistics for simple particles, the degeneracy of arrangements of polyatomic species is strongly influenced by the structure of the lattice space. On the other hand, RSA

*cornette@unsl.edu.ar

of particles of different sizes and shapes on solid surfaces is a subject of considerable practical importance [39,40]. In [19,41] and [42], the percolation behavior of an RSA of linear segments with different size and the percolation of dissociative dimers have been studied, respectively. More recently, the percolation of k-mers with different structures and shapes deposited on a square lattice has been discussed [43–46]. In the cases above, the dependency of the percolation threshold with the parameters of the problem and the universality of the phase transition present in the system have been discussed. In particular, it is interesting to note that for different k-mers, the spanning cluster has the same fractal dimension, d_f. However, the percolation clusters present morphological differences according to the percolating species from which they originated.

The main aims of the present paper are (i) to determine how the RSA process is affected when the surface presents a particular heterogeneity, i.e., the substrate considered is a fractal, and (ii) to draw different criteria from characterizing the fractal surface by means of the RSA process.

The remainder of this paper is organized as follows. Section II describes the models and the substrates on which the irreversible process is studied. Section III presents the results and discussion of the simulations, while the conclusions are provided in Sec. IV.

II. THE MODEL

The system consists of both extended particles and fractal substrates on which those particles are being adsorbed. The adsorbed particles are assumed to be composed of k identical units arranged in two types of configurations: (i) as a linear array of monomers, which is called *linear* k-mers, and (ii) as L-shaped. The adsorption is random and sequential, which means that at any time one particle may be positioned randomly (at random position and orientation). The particles cannot overlap, so when overlapping is detected, the trial of adsorption of the given particle is rejected and the next position and orientation are randomly generated (RSA standard model). Once the particle lands in an empty space, it stays there forever. Two different types of fractals are considered as a substrate: (a) deterministic and (b) statistical; they are described below in this section. The main quantities considered in this paper are the jamming coverage, θ_j, and the temporal evolution parameter, σ, for each case; they are calculated by considering Eq. (1). Both quantities will be affected by the morphology of the adsorbent that is characterized through the average coordination number.

A. Deterministic fractals

Sierpinski carpets of different patterns are considered to be deterministic fractals. They are a special kind of two-dimensional fractals that are determined by a generator. This generator is a square divided in $L \times L$ identical subsquares; then, l^d of these are removed and $l' = L^d - l^d$ are kept (d is the space dimension). In the next step of iteration, each one of these kept squares (not removed) will be subdivided in $L \times L$ identical subsquares, and the pattern of the generator is repeated on these. This construction process is infinitely repeated, generating Sierpinski carpets of fractal dimension given by

$$d_f = \frac{\ln(l')}{\ln L}. \tag{2}$$

Due to the simple generation rule, the Sierpinski carpet can be built in different patterns with different fractal dimension (d_f) and others properties. In Fig. 1, some patterns labeled SC(L,l) are shown as an example of the fractals used in the present work.

B. Statistical fractals

Here, it is shown how the statistical fractals used as substrates are built. A periodic square lattice of linear size N on which polyatomic species are deposited at random is considered. For such particle deposition, the next scheme is followed. If a polyatomic particle formed by h units is considered for deposition, an h-uple of nearest-neighbor sites is randomly selected; if it is vacant, the h-mer is then deposited on those sites. Otherwise, the attempt is rejected. In any case, the procedure is iterated until N' h-mers are deposited and the desired concentration (given by $p = hN'/N^2$) is reached. As is well known, an important goal of the percolation theory is based on finding the minimum concentration p for which a cluster (a group of occupied sites in such a way that each site has at least one occupied nearest-neighbor site) extends

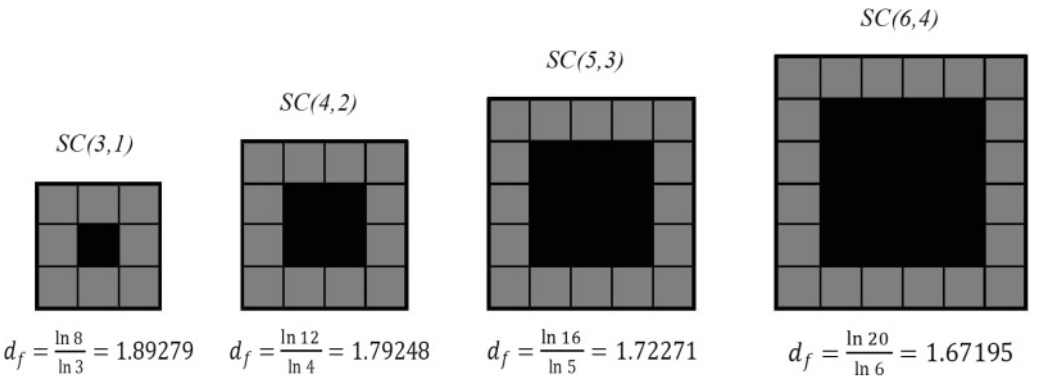

FIG. 1. Different patterns of the Sierpinski carpets used in the present work.

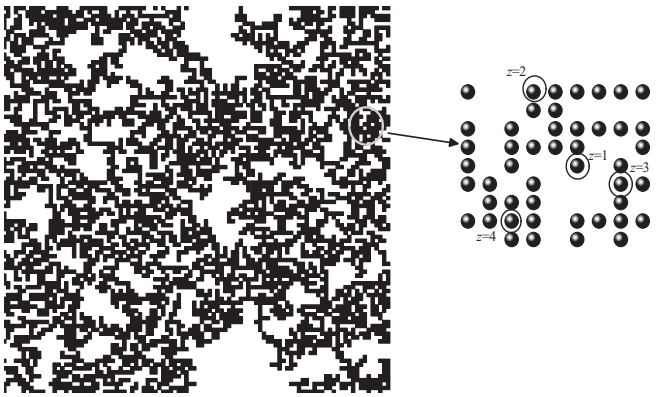

FIG. 2. Percolation cluster generated from polyatomic species. Inset in the figure is an enlargement of a small part of the spanning cluster, which illustrates the variation of the coordination number (z) in the fractal substrates.

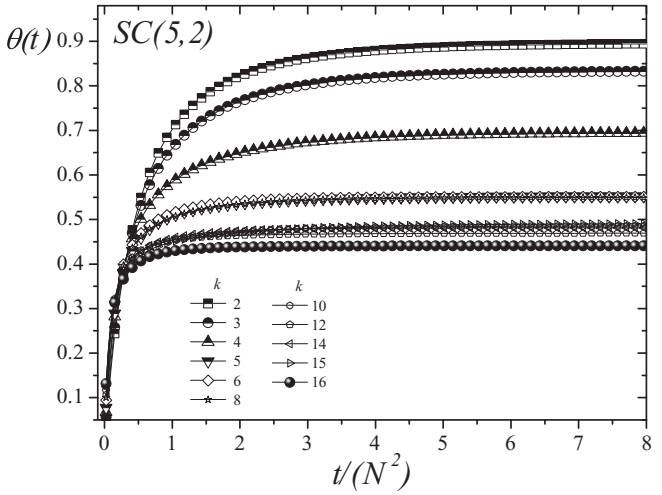

FIG. 3. Coverage as a function of t for different linear k-mer sizes on SC(5,3).

from one side to the opposite side of the system [indeed, there exists a finite probability of finding $n(>1)$ spanning clusters [47–50]]. This particular value of the concentration rate is called the critical concentration or percolation threshold (p_c), and it determines a phase transition in the system. In the random percolation model, a single site is occupied with probability p. In that case, a continuous phase transition appears at p_c that is characterized by well-defined critical exponents. This mapping to critical phenomena made percolation a full part of the theoretical framework of collective phenomena and statistical physics [51–54]. The spanning clusters obtained by using the standard Hoshen and Kopelman algorithm [55] were used in the present paper as statistical fractals, while in [43,44] details of the evolution of the percolation threshold with h were presented.

These fractal surfaces (the spanning clusters) as well as the deterministic ones introduced above present intrinsic heterogeneities due to the fact that their coordination number (z) depends locally on each sites of deposition. In Fig. 2, a sample of such substrates can be observed in detail. As a consequence, there exists an average coordination number ($\langle z \rangle$) that characterizes each fractal.

III. RESULTS AND DISCUSSIONS

A. Sierpinski carpet

RSA of *linear* and L-shaped k-mers of several sizes was studied by Monte Carlo simulations on the patterns shown in Fig. 1. The time evolution of coverage toward the jamming state was calculated for each case. In Fig. 3, the functionality of $\theta(t)$ for different k-mer sizes on SC(5,3) can be observed. Other patterns present a similar behavior. It can be clearly observed that the late-stage deposition kinetics on these kinds of heterogeneous surfaces follows an exponential law, such as the well-known simple deposition on homogenous substrates, Eq. (1).

This behavior allows us to calculate σ, which gives information in relation to the time of adsorption process for each case. Thus, σ can be evaluated by a linear fit from the slope of the curve $\ln[\theta_j - \theta(t)]$ as a function of t.

Mathematic fractals are obtained after an infinite number of step iterations (K), while in the simulation, a fractal is made by means a finite numbers of K. In the studied cases, due to the computational requirements, different step iterations (K) have been used for each pattern. These are summarized in Table I, where N is the lattice linear size given to L^K.

The results for the deposition process of linear k-mers of different sizes on the substrate characterized by SC(3,1), SC(4,2), SC(5,3), SC(6,4), and SC(7,5) will be presented. The jamming coverage as a function of species size, k, for different patterns is shown in Fig. 4.

It can be observed that θ_j decreases as the k-mer's size increases. However, note that $k \cong L$ (which characterizes the pattern-generating cell), and θ_j presents a deep decrement that is more evident in patterns with greater L, such as SC(6,4) and SC(7,5) (Fig. 4). This behavior can be understood if one considers that k-mers whose sizes are smaller than L are able to fill up the lattice in a more dense way without leaving so many holes. In contrast, when the size of the species is greater than or equal to L, these require more free sites for deposition, and the final result is a distribution that is less dense, with more empty sites found.

The results obtained by calculating the σ^{-1} parameter for the different cases studied are presented in Fig. 5. Unlike the behavior found so far, it appears that the value of σ^{-1} presents an oscillation when this is plotted as a function of the species size. It is interesting to note that for each pattern studied, minimum values appear, as indicated in

TABLE I. Patterns, step iterations, and linear size of Sierpinski carpets used in the present paper.

Pattern	Step iteration (K)	Linear size N
3 SC(3,1)	7	2187
4 SC(4,2)	5	1024
5 SC(5,3)	4	625
6 SC(6,4)	4	1296
7 SC(7,5)	4	2401

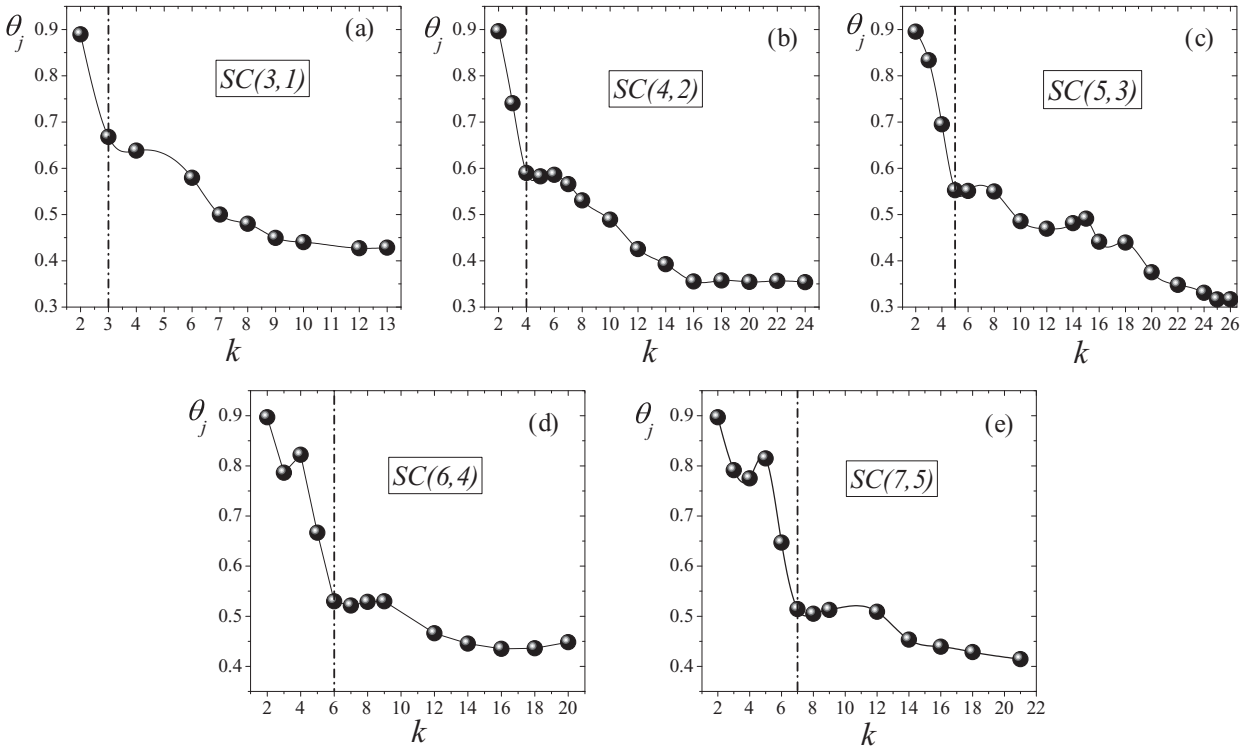

FIG. 4. Jamming coverage as a function of linear k-mer size on different patterns as indicated (the lines are simply a guide for the eyes).

Fig. 5 (gray dots), only in multiples of L (which characterizes each pattern). For example, for the surface characterized by $L = 3$, minima occur when the linear species take the values $k = 3, 6, 9, 12$, etc. For these k-mers, the time evolution toward the jamming state is longer than that for the other species size.

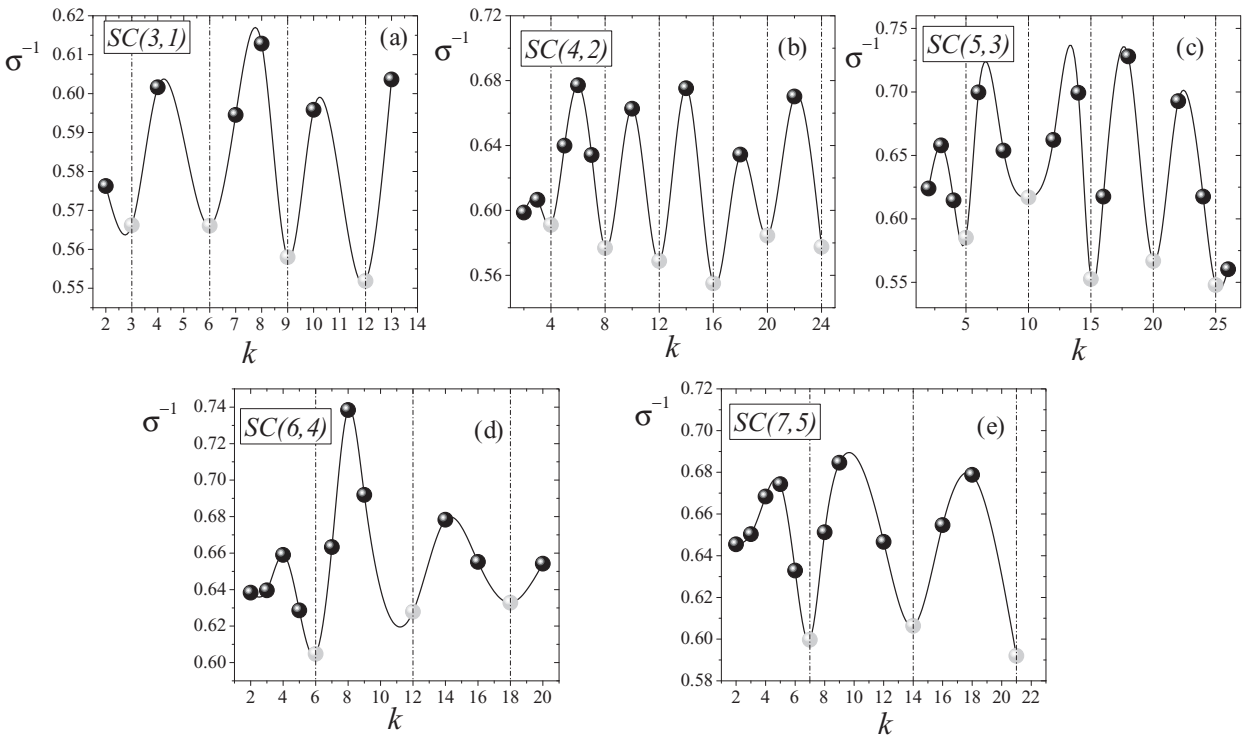

FIG. 5. σ^{-1} as a function of k for different Sierpinski carpets as indicated (the lines are simply a guide for the eyes).

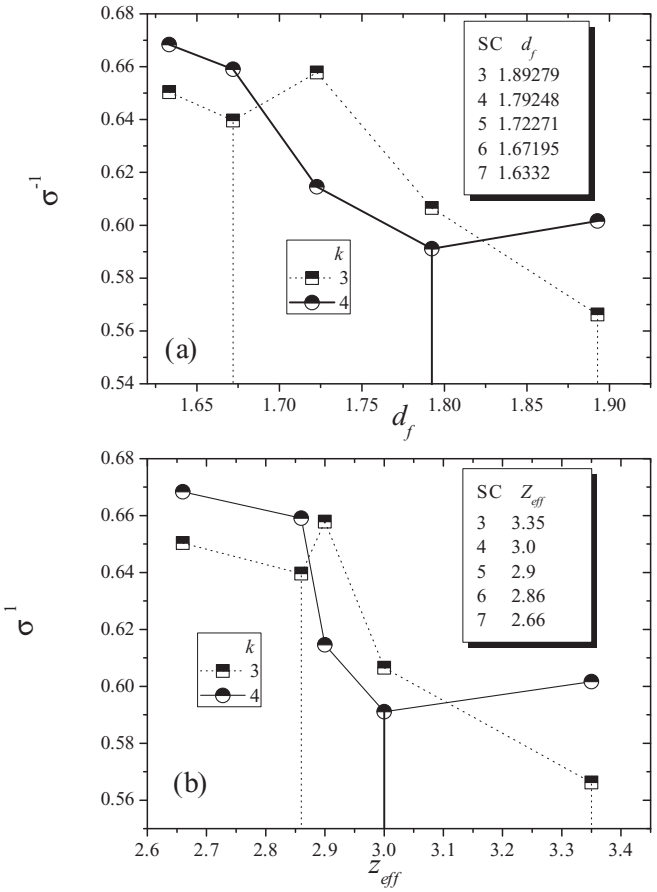

FIG. 6. σ^{-1} as a function of both (a) the fractal dimension of the surface and (b) the mean coordination number of the carpet for $k = 3$ and 4 as indicated. The vertical lines reflect the cases in which k is a multiple of L.

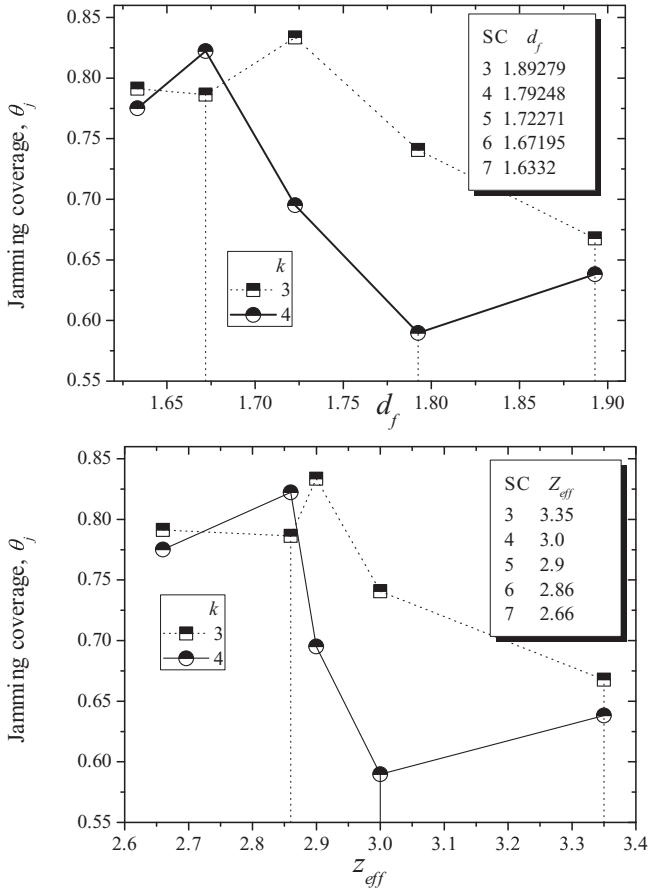

FIG. 7. Jamming coverage θ_j as a function of both (a) the fractal dimension of the surface and (b) the mean coordination number of the carpet for $k = 3$ and 4 as indicated. The vertical lines reflect the cases in which k is a multiple of L.

To make more evident the connection between the geometric aspect of the depositing particles and the substrate, the behavior of the parameter that describes the RSA process (σ^{-1} and the jamming coverage) is plotted as a function of both the fractal dimension of the surface and the mean coordination number of the carpets. The fractal dimension is determined as in Fig. 1. The mean number $z_{\text{eff}}(l_d; N_{\text{occ}}; K)$ of nearest neighbors per site with periodic boundary conditions provides a convenient measure of the mean local topology of these structures and their convergence speed toward the thermodynamic limit. It can be shown that [56–58]

$$z_{\text{eff}}(l^d; N_{\text{occ}}; K) = \frac{N_I}{N_{\text{occ}} - N_S}\left[1 - \left(\frac{N_S}{N_{\text{occ}}}\right)^K\right] + \left(\frac{N_S}{N_{\text{occ}}}\right)^K d, \tag{3}$$

where N_S is the number of occupied sites on each hypersurface of the generating cell, N_I is the number of its internal bonds, l is the size of the generating cell, d is the dimension of embedding space, and N_{occ} is the number of occupied sites in the generating cell. The lattice is generated by enlarging the $(K-1)$th iteration one by replacing each occupied site by the whole generating cell. Strictly speaking, a Sierpinski lattice is not a true fractal except that K tends to infinity.

Figures 6(a) and 6(b) shows that σ^{-1} grows upon decreasing the fractal dimension and the mean coordination number (here, only the cases $k = 3$ and 4 are shown). However, it is important to emphasize that σ^{-1} presents relative minima when the depositing species coincides with a multiple of L, which characterizes each pattern. For the studied cases, the minima appear for $L = 3$ and $L = 6$ ($L = 4$) in the case of $k = 3$ ($k = 4$), which are shown by vertical lines in the figures. Similar conclusions can be drawn from Figs. 7(a) and 7(b), where the jamming coverage is plotted for the same conditions as in Fig. 6. Both graphics show that the kinetic parameters that determine the properties of the RSA of polyatomic species on fractal structures are strongly influenced by both the main characteristic of the surface where the particles are deposited and the size of the k-mers.

1. L-shaped deposition

One may now be interested in studying how the k-mer–geometry relation affects the RSA process. For this purpose, the L-shaped deposition on Sierpinski carpets is analyzed by calculating the main parameters θ_j and σ for different patterns. In Figs. 8 and 9, the results obtained for all cases studied are shown.

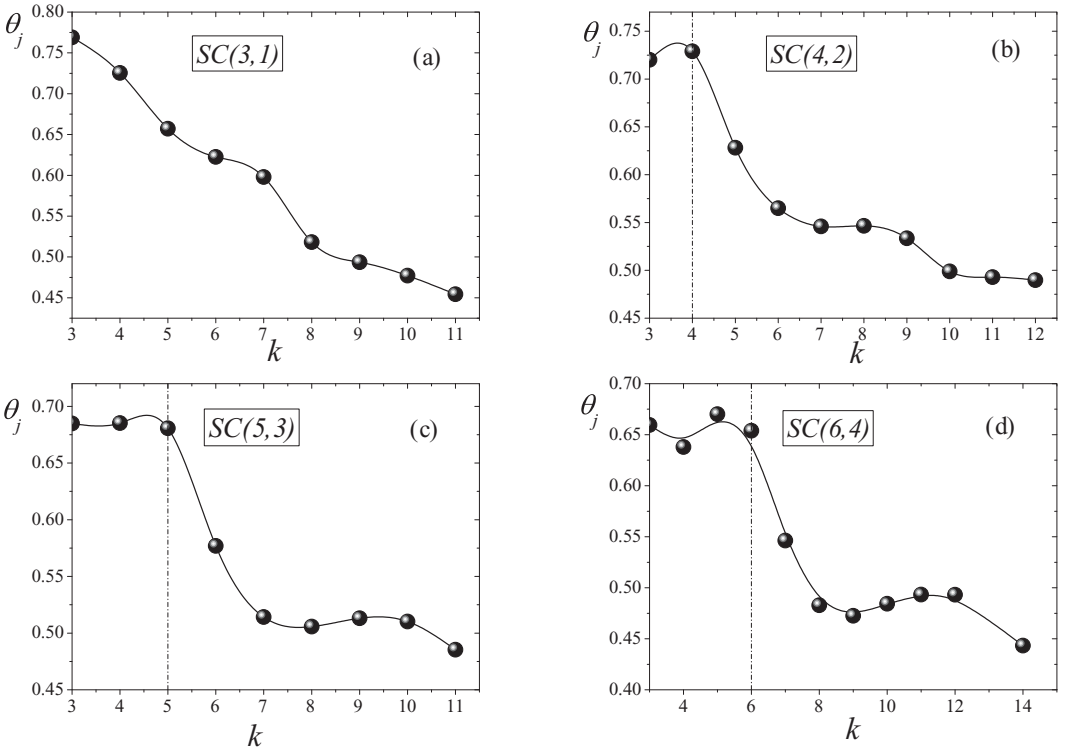

FIG. 8. Jamming coverage as a function of L-shaped k-mer sizes on different patterns as indicated (the lines are simply a guide for the eyes).

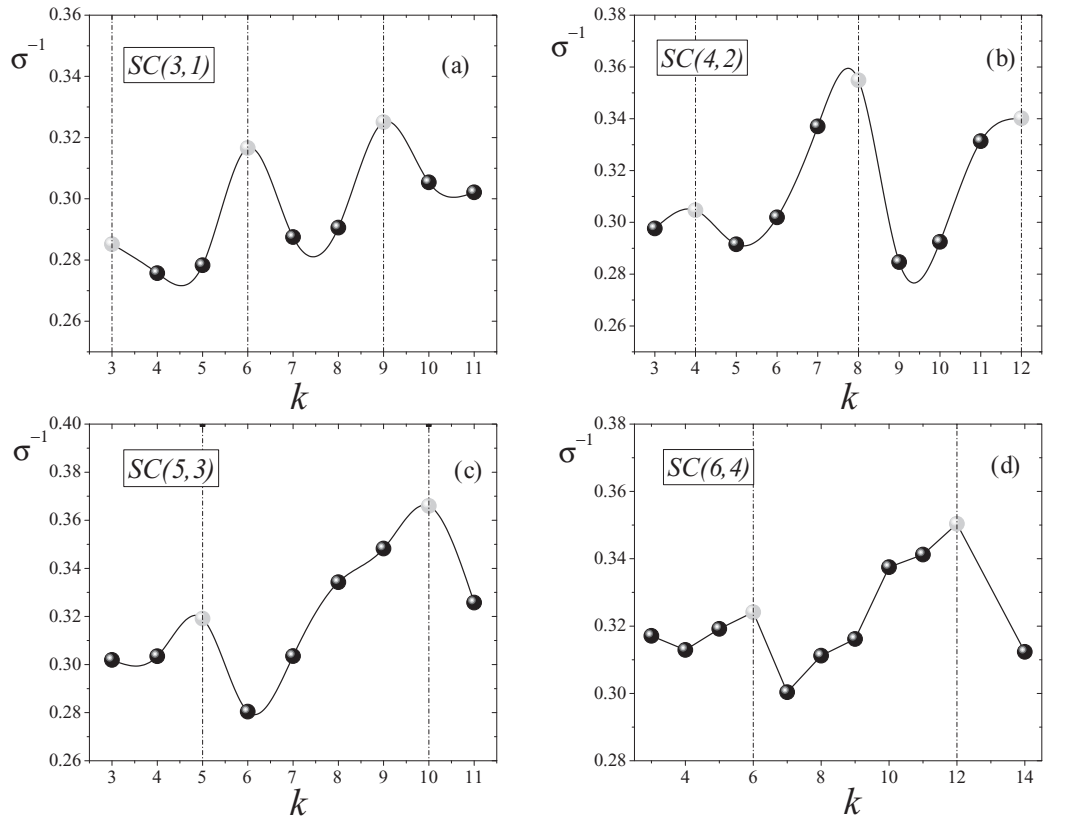

FIG. 9. σ^{-1} as a function of k for the different structures as indicated (the lines are simply a guide for the eyes).

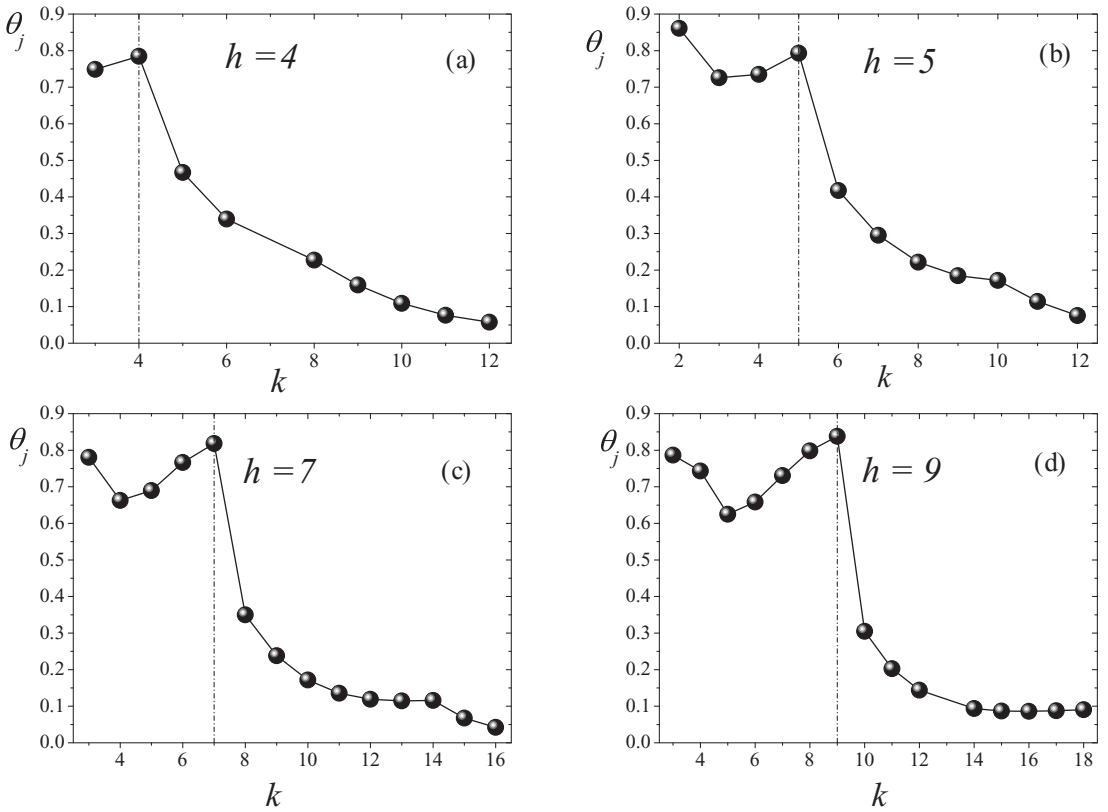

FIG. 10. Jamming coverage as a function of k for linear k-mers deposited on spanning clusters formed from linear species of h size. The lines are simply a guide for the eyes.

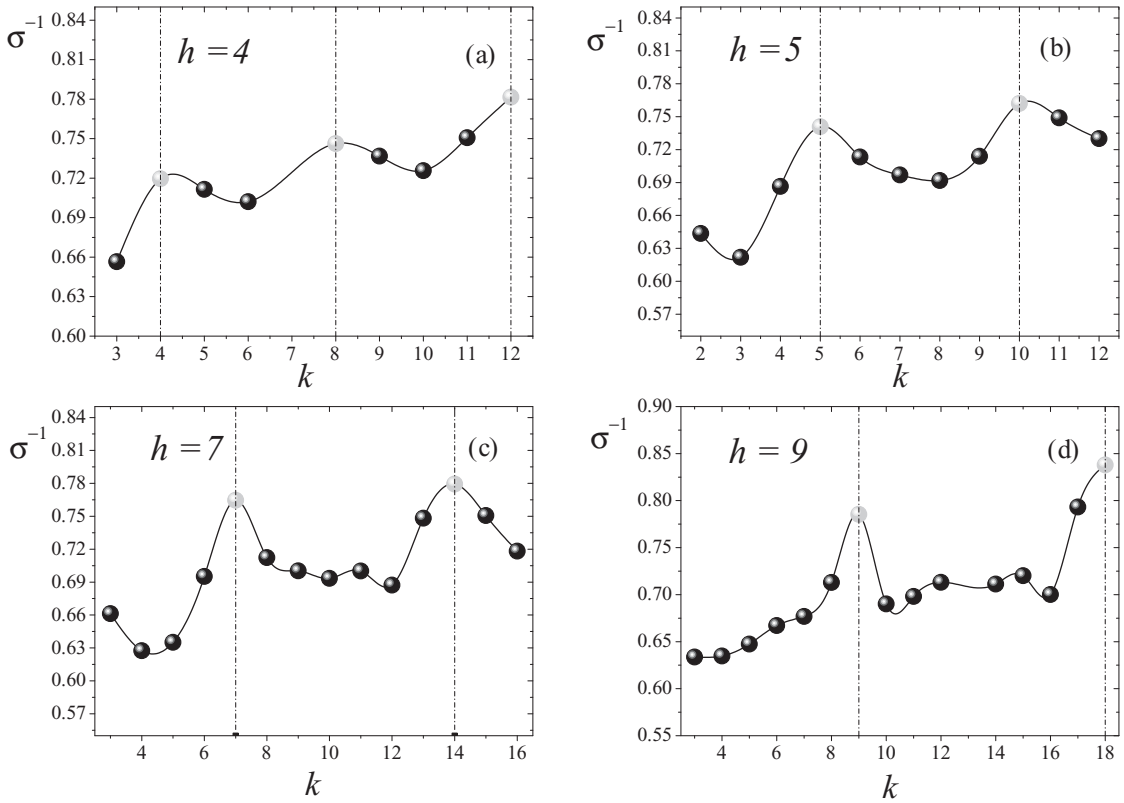

FIG. 11. σ^{-1} for different k-mer sizes (the lines are simply a guide for the eyes).

The RSA of L-shaped deposition on this kind of deterministic fractal presents the same behavior as that of linear k-mers. However, notice that a significant decrease of jamming coverage occurs when the k-mer sizes are greater than L, unlike the linear case in which θ_j declines just for the k-mer size $\cong L$.

The results for σ^{-1} obtained after properly fitting from $\ln[\theta_j - \theta(t)]$ versus $t/(N^2)$ by Monte Carlo simulation are presented in Fig. 9. An oscillating behavior can be observed for the σ^{-1} parameter as a function of k-mer size. While minima were observed for linear species, maxima appear when the size of the species is just a multiple of L. It should be noted that the kinetics of deposition depends on the degree of freedom of the species, and L-shaped k-mers have a different dynamics [59] from that of the linear particles. The increase in the value of the parameter σ^{-1} indicates that the processing times are shorter in these cases.

B. Spanning clusters of polyatomic species

Here, a similar analysis as discussed before will be performed on statistical fractals. In this study, spanning clusters of polyatomic species are used as substrates for the RSA process of linear k-mers. As was mentioned above, these surfaces that have been studied in previous works [43,44] are generated from the random deposition process of polyatomic species. In this study, our goal is to explore how the RSA process is modified by the symmetry of a substrate.

Also considered is the study of RSA for linear h-mers on a spanning cluster formed by linear and tortuous h-mers [self-avoiding random walk (SAW) of length h)] for a given size h. For clarity, h has been designated to identify the size of the species that have formed the substrate, and k has been reserved to refer to the size of the species involved in the process of RSA on those surfaces.

The time evolution of the surface coverage in these kinds of fractals presents the exponential behavior given by Eq. (1). This dependence allows us to calculate, as was done previously, the σ parameter from an appropriate linear fit.

1. Percolation clusters from linear polyatomic species

The jamming coverage was calculated for different surfaces originating from linear h-mer deposition characterized by $h = 4$, 5, 6, 7, and 9. In Fig. 10, θ_j is presented as a function of k (where k refers to the species involved in the RSA process). A well-defined maximum can be observed when the k-mer size coincides with the size of the species that formed the surface. The same behavior was observed above for deterministic fractals, and it demonstrates a clear dependence on the adsorbent structure.

The calculated values of σ^{-1} are presented in Fig. 11. An oscillating behavior was again found as a function of the adsorbed k-mer size, analogous to Sierpinski carpets. The gray dots indicate peaks in σ^{-1} values, which emphasize that these are produced, such as in the Sierpinski carpets, when the k-mer size is a multiple of the h-mer generator.

It should be noted that these fractal surfaces have the same fractal dimension, d_f, as in the case of a percolation of monomers [43]. It is, therefore, of great interest to be able to find quantities to describe them.

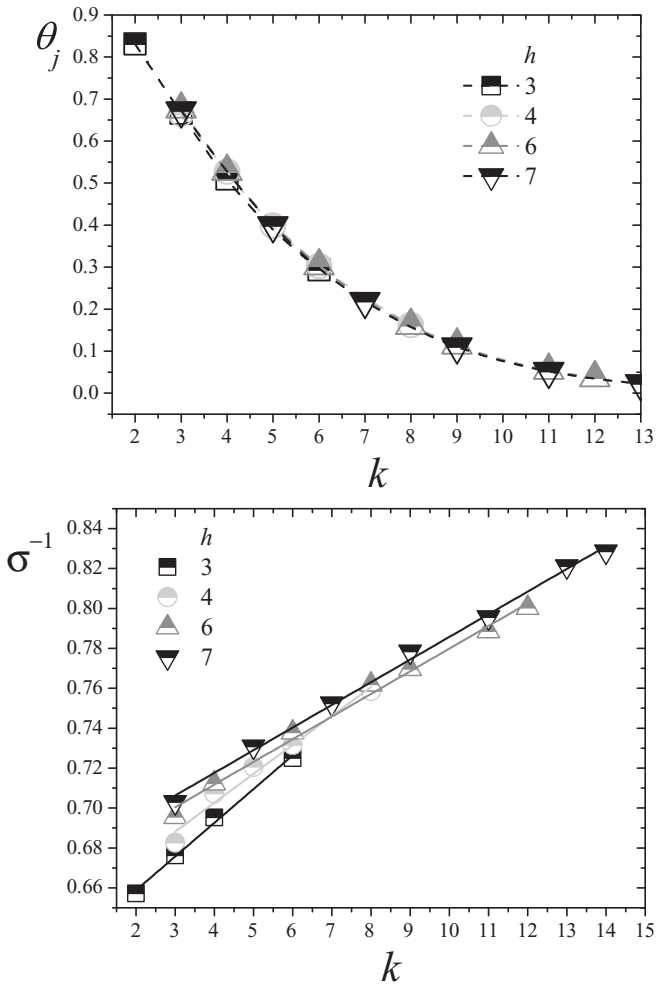

FIG. 12. (a) Jamming coverage as a function of k for linear k-mers deposited on spanning clusters formed from SAW species of h size. (b) σ^{-1} as a function of k for different substrate characterized for h. The lines are simply a guide for the eyes.

From the analysis of the quantities presented in the present paper, it can be observed that this type of surface with well-defined geometry has a significant effect on the irreversible deposition process, which is reflected in both the limiting jamming, θ_j, and the time of deposition, σ.

2. Percolation clusters from SAW polyatomic species

The behavior observed in both deterministic and statistical fractals (formed from linear h-mers) shows a clear dependence between the geometry of the adsorbent and the adsorbate. To gain a deeper understanding of this behavior, the deposition of linear k-mers on percolation clusters formed by SAW species is studied. The results obtained for the jamming coverage are presented in Fig. 12(a), where h indicates that the surface was generated from species including all possible shapes of a determinate size.

From this analysis, it can be observed that the jamming coverage, θ_j, is independent of the adsorbent where the deposition takes place, and it presents a monotonic decrease as the size of the adsorbed species increases. Therefore, a

measure of this quantity provides poor information about the adsorbate as well as the adsorbent.

In Fig. 12(b), the values obtained for σ^{-1} are presented for each case. A clear linear dependence can be observed for σ^{-1} as a function of the size of the adsorbed species. Although this linear behavior presents different fitting parameters for clusters formed from various SAW h-mer sizes, it does not provide enough information to characterize the species involved in the process. All of the reported dates were obtained by Monte Carlo simulation as a result of an average performed on 10^3 samples of percolation clusters generated, for each case (size and shape of h-mer), on square lattices of linear size $N = 1000$. In these spanning clusters, 5×10^3 independent runs were realized for each deposition.

IV. CONCLUSIONS

The study of random sequential and irreversible deposition was performed on two types of fractal substrates: deterministic and statistical. As deterministic fractals, several Sierpinski carpets characterized by different fractal dimensions and topologies were used. Percolation clusters formed from polyatomic species of different shapes and sizes (linear and SAW) were selected as statistical fractals, which have the same fractal dimension as in the simple percolation case [43,44].

The main results were as follows: (a) The jamming coverage, θ_j, presents a significant decrement when the deposited linear k-mer size coincides with L (which characterizes the generator cell), and for the L-shaped case it decreases when the species size is greater than L. The same behavior is found for spanning clusters formed from linear h-mers ($>h$). (b) The time evolution parameter σ^{-1} presents oscillations (minima and maxima) as a function of the adsorbed particle size. These minima (maxima) appear when the size of the particle is a multiple of L (L in the L-shaped k-mers case and h for linear spanning clusters). (c) In the case of percolation clusters formed from SAW h-mers, the main parameters (θ_j and σ^{-1}) provided very poor information with regard to the substrate-adsorbate geometry.

The results mentioned in points (a) and (b) allow us to conclude that the RSA process on heterogeneous surfaces, which introduce symmetry (such as deterministic or statistical fractals formed from species that introduce symmetry to the surface), enables us to identify either the substrate (when the adsorbed particle is known) or the adsorbed species (when the adsorbent is known). In addition, these results suggest a strategy for the identification and characterization of surfaces or the deposited particles by means of experiments.

ACKNOWLEDGMENTS

This work was supported in part by CONICET (Argentina) under project PIP 112-200801-01332, Universidad Nacional de San Luis (Argentina) under project 322000, and the National Agency of Scientific and Technological Promotion (Argentina) under project 33328 PICT 2005. The numerical work was done using the BACO parallel cluster located at Instituto de Física Aplicada, Universidad Nacional de San Luis - CONICET, San Luis, Argentina.

[1] P. J. Flory, J. Am. Chem. Soc. **61**, 1518 (1939).
[2] A. C. Balazs and I. R. Epstein, Biopolymers **23**, 1249 (1984).
[3] A. Cordoba and J. J. Luque, Phys. Rev. B **31**, 8111 (1985).
[4] V. Privman, H. L. Frish, N. Ryde, and E. Matijvec, J. Chem. Soc., Faraday Trans. **87**, 1371 (1991).
[5] Z. Adamczyk, T. Babros, J. Czarnecki, and T. G. M. van de Ven, Adv. Colloid Interface Sci. **19**, 183 (1983).
[6] L. Finegold and J. T. Donnell, Nature (London) **278**, 443 (1979).
[7] J. W. Evans, D. E. Sanders, P. A. Thiel, and A. E. DePristo, Phys. Rev. B **41**, 5410 (1990).
[8] J. Fransaer, Ph.D. thesis, Katholieke Universiteit Leuven (1994).
[9] N. Provatas, M. Haataja, E. Seppälä, S. Majaniemi, J. Å. Ström, M. Alava, and T. Ala Nissila, J. Stat. Phys. **87**, 385 (1997).
[10] K. Trojan and M. Ausloos, Physica A **351**, 332 (2005).
[11] L. Zhang and P. R. Van Tassel, J. Chem. Phys. **112**, 3006 (2000).
[12] M. Hasegawa and M. Tanemura, in *Recent Developments in Statistical Inference and Data Analysis*, edited by K. Matusita (North-Holland, Amsterdam, 1980).
[13] Y. Itoh, J. Appl. Probab. **17**, 134 (1980).
[14] M. Nakamura, Phys. Rev. A **36**, 2384 (1987).
[15] P. Schaaf and J. Talbot, Phys. Rev. Lett. **62**, 175 (1989).
[16] R. D. Vigil and R. M. Ziff, J. Chem. Phys. **91**, 2599 (1989).
[17] J. Talbot, G. Tarjus, and P. Schaaf, Phys. Rev. A **40**, 4808 (1989).
[18] J. D. Sherwood, J. Phys. A **23**, 2827 (1990).
[19] B. Bonnier, M. Hontebeyrie, Y. Leroyer, C. Meyers, and E. Pommiers, Phys. Rev. E **49**, 305 (1994).
[20] A. Baram and M. Fixman, J. Chem. Phys. **103**, 1929 (1995).
[21] J. Evans and R. S. Nord, J. Stat. Phys. **38**, 681 (1985).
[22] N. Nazemifard, J. H. Masliyah, and S. Bhattacharjee, J. Colloid Interface Sci. **293**, 1 (2006).
[23] N. Nazemifard, J. H. Masliyah, and S. Bhattacharjee, Langmuir **22**, 9879 (2006).
[24] A. Cadilhe and V. Privman, Mod. Phys. Lett. B **18**, 207 (2004).
[25] N. A. M. Araújo, A. Cadilhe, and V. Privman, Phys. Rev. E **77**, 031603 (2008).
[26] H. Zheng, M. F. Rubner, and P. T. Hammond, Langmuir **18**, 4505 (2002).
[27] I. Karakurt, P. Leiderer, and J. Boneberg, Langmuir **22**, 2415 (2006).
[28] X. Jiang, H. Zheng, S. Gourdin, and P. T. Hammond, Langmuir **18**, 2607 (2002).
[29] C. Kruger and U. Jonas, J. Colloid Interface Sci. **252**, 331 (2002).
[30] R. Michel, J. W. Lussi, G. Csucs, I. Reviakine, G. Danuser, B. Ketterer, J. A. Hubbell, M.T extor, and N. D. Spencer, Langmuir **18**, 3281 (2002).
[31] J. Y. Chen, J. K. Klemic, and M. Elimelech, Nano Lett. **4**, 393 (2002).
[32] K. M. Chen, X. Jiang, L. C. Kimerling, and P. T. Hammond, Langmuir **16**, 7825 (2000).

[33] H. Fudouzi, M. Kobayashi, and N. Shinya, Langmuir **18**, 648 (2002).
[34] H. Zheng, M. C. Berg, M. F. Rubner, and P. T. Hammond, Langmuir **20**, 7215 (2004).
[35] J. Rundqvist, J. H. Hoh, and D. B. Haviland, Langmuir **22**, 5100 (2006).
[36] S. Liang, M. Chen, Q. Xue, Y. Qi, and J. Chen, J. Colloid Interface Sci. **311**, 104 (2007).
[37] N. Elimelech, J. Y. Chen, and Z. A. Kuznar, Langmuir **19**, 6594 (2003).
[38] J. Wright, E. Ivanowa, D. Pham, L. Filipponi, A. Viezzoli, K. Suyama, M. Shirai, M. Tsunooka, and D. V. Nicolau, Langmuir **19**, 446 (2003).
[39] J. Evans, Rev. Mod. Phys. **64**, 1281 (1993).
[40] V. Privman, J.-S. Wang, and P. Nielaba, Phys. Rev. B **43**, 3366 (1991).
[41] Y. Leroyer and E. Pommiers, Phys. Rev. B **50**, 2795 (1994).
[42] Z. Gao and Z. R. Yang, Physica A **255**, 242 (1998).
[43] V. Cornette, A. J. Ramirez-Pastor, and F. Nieto, Physica A **327**, 71 (2003).
[44] V. Cornette, A. J. Ramirez-Pastor, and F. Nieto, Eur. Phys. J. B **36**, 391 (2003).
[45] M. Dolz, F. Nieto, and A. J. Ramirez-Pastor, Phys. Rev. E **72**, 066129 (2005).
[46] V. Cornette, A. J. Ramirez-Pastor, and F. Nieto, J. Chem. Phys. **125**, 204702 (2006).
[47] M. Aizenman, Nucl. Phys. B **485**, 551 (1997).
[48] J. Cardy, J. Phys. A **31**, L105 (1998).
[49] L. N. Shchur and S. S. Kosyakov, Int. J. Mod. Phys. C **8**, 473 (1997).
[50] L. N. Shchur, *Spanning Clusters in Square and Cubic Percolation*, in Springer Proceedings in Physics, Vol. 85, edited by D. P. Landau, S. P. Lewis, and H. B. Schuettler (Springer Verlag, Heidelberg, 2000).
[51] A. Coniglio, Nucl. Phys. A **681**, 451 (2001).
[52] C. M. Fortuin and P. W. Kasteleyn, Physica **57**, 536 (1972).
[53] P. W. Kasteleyn and C. M. Fortuin, J. Phys. Soc. Jpn. Suppl. **26**, 11 (1969).
[54] S. Fortunato, Phys. Rev. B **66**, 054107 (2002); **67**, 014102 (2003).
[55] J. Hoshen and R. Kopelman, Phys. Rev. B **14**, 3428 (1976).
[56] P. Y. Hsiao, P. Monceau, and M. Perreau, Phys. Rev. B **62**, 13856 (2000).
[57] P. Monceau and M. Perreau, Phys. Rev. B **63**, 184420 (2001).
[58] M. Perreau and J. C. S. Levy, Phys. Rev. A **40**, 4690 (1989).
[59] V. Cornette, D. Linares, A. J. Ramirez-Pastor, and F. Nieto, J. Phys. A **40**, 11765 (2007).